Self-Assembly and Waterlike Anomalies in Janus Nanoparticles

José Rafael Bordin,[*,†] Leandro B. Krott,[*,‡] and Marcia C. Barbosa[*,¶]

Campus Caçapava do Sul, Universidade Federal do Pampa, Av. Pedro Anunciação, 111, CEP 96570-000, Caçapava do Sul, RS, Brazil, Campus Araranguá, Universidade Federal de Santa Catarina, Rua Pedro João Pereira, 150, CEP 88900-000, Araranguá, SC, Brazil, and Instituto de Física, Universidade Federal do Rio Grande do Sul, Caixa Postal 15051, CEP 91501-970, Porto Alegre, RS, Brazil

E-mail: josebordin@unipampa.edu.br; leandro.krott@ufsc.br; marciabarbosa@ufrgs.br

Abstract

We explore the pressure versus temperature phase diagram of a system of dimeric Janus nanoparticles using Molecular Dynamics simulations. Each nanoparticle is modeled as a dumbbell which has one monomer that interacts by a standard Lennard-Jones potential while the other monomer interacts by a core-softened potential. The systems composed by particles interacting only by core-softened potential exhibit the density and the diffusion anomalous behavior observed in water while if the particles interact only by the Lennard-Jones potential no anomaly is present. Here we explore if the anomalous behavior is present when half of the particles are modeled by a core-softened

[*]To whom correspondence should be addressed

[†]Campus Caçapava do Sul, Universidade Federal do Pampa, Av. Pedro Anunciação, 111, CEP 96570-000, Caçapava do Sul, RS, Brazil

[‡]Campus Araranguá, Universidade Federal de Santa Catarina, Rua Pedro João Pereira, 150, CEP 88900-000, Araranguá, SC, Brazil

[¶]Instituto de Física, Universidade Federal do Rio Grande do Sul, Caixa Postal 15051, CEP 91501-970, Porto Alegre, RS, Brazil

potential and half with Lennard-Jones potential. We show that the diffusion anomaly is preserve, while the density anomaly can disappear depending on the non-anomalous monomer characteristics. We also show that the self-assembly structures characteristics of the dumbbell systems are affected by the balance between core-softened and non-core-softened monomers.

Introduction

The understanding of the structure, dynamic and thermodynamic behavior of the colloidal systems is important not only due to their applications in medicine, catalysis, production of photonic crystals, stable emulsions[1–3] but also for the understanding of the biomolecules.[4]

One of the relevant characteristics of the colloidal solutions is the formation of stable self-assembly structures not present in traditional molecular systems.[5,6] In principle the agglomeration of the colloids when in solution with smaller solvent particles arises from the entropic depletion forces. However, the structures formed depend on the size and shape of the colloid, as well as, on the colloid-colloid and the colloid-solvent interactions. Therefore, understanding the microscopic mechanism for the formation of the self-assembly structures allow for using the colloids as the building blocks into a desired mesoscopic structure and function.

The colloids with the dumbbell shape are quite particular. Each dumbbell is a dimer formed by two spheres with the same diameter that overlap with a separation that varies from an almost total overlap to one or two monomer diameters. In this case the anisotropic anisotropy plays quite a relevant role. The properties of the system depend on the interaction potential that varies with their spatial separation and their relative orientations.

In this case a more elaborated interaction potential can lead to a more complex phase diagram. Two length scales potentials are characterized by having two preferred particle-particle distances, while one length scale potentials, as the standard Lennard Jones potential, shows only one preferred distance. One specific type of two-length scale potential is the

core-softened (CS) potential. For instance, the increase of density with the temperature at a fixed pressure and the increase of diffusivity under compression are examples of these anomalies. Water is the most well known fluid that present thermodynamic, dynamic and structural anomalous behavior,[7–9] with 72 known anomalies.[10] In addition, silicon[11] and others material, as silica,[12–14] Te,[15] Bi,[16] Si,[17,18] $Ge_{15}Te_{85}$,[19] liquid metals,[20] graphite[21] and BeF_2[12] shows thermodynamic anomalies,[9] while silicon[22] and silica[11,13,14,23] show a maximum in the diffusion coefficient at constant temperature.

If each monomer of the dumbbell interacts with the other monomer by an one length scale potential, the Lennard-Jones (LJ) potential for instance, the pressure versus temperature phase diagram of the pure dimeric system resembles the phase diagram of the pure monomeric case[24] with no liquid-crystal-like phase present. However, if each monomer of one dumbbell interacts with the other monomer of a different dumbbell by a two length scale potential the dimeric system shows a richer pressure versus temperature phase diagram when compared with the monomeric system, including the presence of a liquid-crystal-like phase.[24] This new phase is characterized by the dimers aligning with the dumbbells diffusing along these lines.[24]

One special type of dumbbell is the Janus particle,[25–30] characterized by having two dissimilar monomers. These different types of monomers can be hydrophobic/hydrophilic,[31–33] charged/neutral[34,35] and metallic/polymer. Even though these dissimilar interactions are individually described by one length scale potential, the competition between attractive and repulsive forces lead to the formation of self-assembly lamellar or micellar phases.[36–38]

Recently, the production of silver-silicon (Ag-Si) hybrid Janus dimers was reported.[26] The silver-silver interaction can be described by an one length scale potential and consequently the pure silver system does not show the presence of the water-like thermodynamic and dynamic anomalies. Silicon, however, is classified as an anomalous fluid and the silicon-silicon interaction in the pure system is modeled by a two length scale potential, namely a core-softened potential

Then, the question of what happens with the pressure versus temperature phase diagram

of a Janus dumbbell system composed by the combination of one type of monomer that interacts by a core-softened potential and another type of monomer that interacts by an one length scale potential? At one hand the two length scales favors the formation of liquid-crystal-like structures, and in the other hand the presence the two different monomers leads to the formation of the lamellar phases.

In order to answer to this question we study the pressure versus temperature phase diagram of two model systems. The first system is a composed by Janus particles in which one monomer interacts through a core-softened potential with a small attractive term and the other monomer interacts through a purely repulsive potential. The second system is a dumbbell in which one monomer interacts through a core-softened potential but the second monomer exhibits a strong attractive potential. The comparison of these two cases might shade some light in the limits of the interactions needed in order to have the formation of the more diffusive liquid-crystal-like phase or of a solid lamellar phase.

The paper is organized as follows. The model is introduced first and the methods and simulation details are described; next the results and discussion are given; and then conclusions are presented.

The Model and the Simulation details

The system consists of N dimeric nanoparticles, in a total of $2N$ monomers. The Janus dumbbells are modeled using two spherical symmetric particles, each with mass m and both with an effective diameter σ, linked rigidly at a distance $\lambda = 0.8$. Three types of monomers were used. Monomers of type A interact with another monomer of type A through a core-softened potential, while monomers of type B interact with another monomer of type B with a purely repulsive potential and monomers of type C interact with another monomer C through an attractive Lennard-Jones potential. The A-A two length scale interaction

potential is defined as[39]

$$\frac{U^{AA}(r_{ij})}{\varepsilon} = 4\left[\left(\frac{\sigma}{r_{ij}}\right)^{12} - \left(\frac{\sigma}{r_{ij}}\right)^{6}\right] + u_0 \exp\left[-\frac{1}{c_0^2}\left(\frac{r_{ij}-r_0}{\sigma}\right)^2\right] \quad (1)$$

where $r_{ij} = |\vec{r}_i - \vec{r}_j|$ is the distance between two A particles i and j. This equation has two terms: the first term is the standard 12-6 LJ potential[40] while the second parcel is a Gaussian centered at r_0, with depth u_0 and width c_0. Using the parameters $u_0 = 5.0$, $c = 1.0$ and $r_0/\sigma = 0.7$ this equation represents a two length scale potential, with one scale at $r_{ij} \equiv r_1 \approx 1.2\sigma$, where the force has a local minimum, and the other scale at $r_{ij} \equiv r_2 \approx 2\sigma$, where the fraction of imaginary modes has a local minimum.[24] The cutoff radius for this potential is $r_c = 4.0$. Despite the mathematical simplicity of this potential, monomeric and dimeric fluids using this shoulder potential exhibit the density, the diffusion, and the response functions anomalies observed in water and other anomalous fluids.[39,41–44]

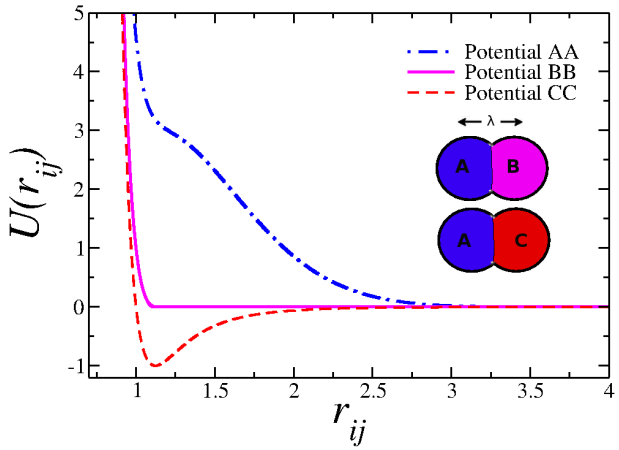

Figure 1: Interaction potentials used in our simulations: the shoulder potential AA (dot-dashed blue line), the CSLJ potential BB with $r_c = 2^{1/6}$ (solid magenta line) and the CSLJ potential CC with $r_c = 2.5$ (dashed red line). Inset: Janus nanoparticles formed by A-B monomers and by A-C monomers.

The B-B repulsive interaction potential is given by a cut and shifted Lennard-Jones

(CSLJ) potential while the C-C attraction is described by a LJ potential namely

$$U^{\mathrm{CSLJ}}(r_{ij}) = \begin{cases} U_{\mathrm{LJ}}(r_{ij}) - U_{\mathrm{LJ}}(r_c) \ , & r_{ij} \leq r_c \ , \\ 0 \ , & r_{ij} > r_c \ . \end{cases} \tag{2}$$

Here, U_{LJ} is the standard 12-6 LJ potential, included in the first term of equation (1), $r_c = 2^{1/6}$ is the cutoff for the B-B interaction while $r_c = 2.5$ is the cutoff for the C-C interaction. The interactions between A-B, B-C and A-C monomers are also purely repulsive given by the equation (2) with $r_c = 2^{1/6}$. The potentials are illustrated in the figure 1. The internal bonds between each dimer remain fixed using the SHAKE algorithm.[45]

Here we explore two model systems. In the first model the nanoparticles are composed by one monomer of the type A and one monomer of the type B, representing the combination of an anomalous fluid with a nonpolarizable hardcore system. In the second case, the dumbbell is modeled by a monomer of type A and one monomer of type C representing a Janus particle in which one monomer is an anomalous fluid and the other is a attractive system. Both cases are illustrated in the inset of the figure 1.

Molecular dynamics simulations is used in order to obtain the pressure versus temperature ($p \times T$) phase diagram. The simulations were performed in the canonical ensemble using the ESPResSo package.[46,47] A total number of 1000 particles (500 dimers) where used. The number density is defined as $\rho = N/V$, where $V = L^3$ is the volume of the cubic simulation box. Standard periodic boundary conditions are applied in all directions. The system temperature was fixed using the Langevin thermostat with $\gamma = 1.0$, and the equations of motion for the fluid particles were integrated using the velocity Verlet algorithm, with a time step $\delta t = 0.01$. We performed 5×10^5 steps to equilibrate the system. These steps are then followed by 5×10^6 steps for the results production stage. To ensure that the system was equilibrated, the pressure, kinetic energy and potential energy were analyzed as function of time, as well several snapshots at distinct simulation times. To confirm our results, in some points we carried out simulations with 2000 and 5000 particles, and essentially the same

results were observed.

To study the dynamic anomaly the relation between the mean square displacement (MSD) with time is analyzed, namely

$$\langle [\vec{r}_{\rm cm}(t) - \vec{r}_{\rm cm}(t_0)]^2 \rangle = \langle \Delta \vec{r}_{\rm cm}(t)^2 \rangle \ , \tag{3}$$

where $\vec{r}_{\rm cm}(t_0) = (x_{\rm cm}(t_0)^2 + y_{\rm cm}(t_0)^2 + z_{\rm cm}(t_0)^2)^{1/2}$ and $\vec{r}_{\rm cm}(t) = (x_{\rm cm}(t)^2 + y_{\rm cm}(t)^2 + z_{\rm cm}(t)^2)^{1/2}$ denote the coordinate of the nanoparticle center of mass (cm) at a time t_0 and at a later time t, respectively. The MSD is related to the diffusion coefficient D by

$$D = \lim_{t \to \infty} \frac{\langle \Delta \vec{r}_{\rm cm}(t)^2 \rangle}{6t} \ . \tag{4}$$

The structure of the fluid was analyzed using the radial distribution function (RDF) $g(r_{ij})$, and the pressure was evaluated with the virial expansion. In order to check if the Janus system shows density anomaly we evaluate the temperature of maximum density (TMD). Using thermodynamical relations, the TMD can be characterized by the minimum of the pressure versus temperature along isochores,

$$\left(\frac{\partial p}{\partial T} \right)_{\rho} = 0 \ . \tag{5}$$

The fluid and micellar region in the $p \times T$ phase diagram were defined analyzing the structure with $g(r_{ij})$, snapshots and the diffusion coefficient D.

In this paper all the physical quantities are computed in the standard LJ units,[40]

$$r^* \equiv \frac{r}{\sigma} \ , \quad \rho^* \equiv \rho \sigma^3 \ , \quad \text{and} \quad t^* \equiv t \left(\frac{\epsilon}{m \sigma^2} \right)^{1/2} \ , \tag{6}$$

for distance, density of particles and time , respectively, and

$$p^* \equiv \frac{p \sigma^3}{\epsilon} \quad \text{and} \quad T^* \equiv \frac{k_B T}{\epsilon} \tag{7}$$

for the pressure and temperature, respectively, where σ is the distance parameter, ϵ the energy parameter and m the mass parameter. Since all physical quantities are defined in reduced LJ units, the * is omitted, in order to simplify the discussion.

Results and Discussion

A-B type nanoparticles

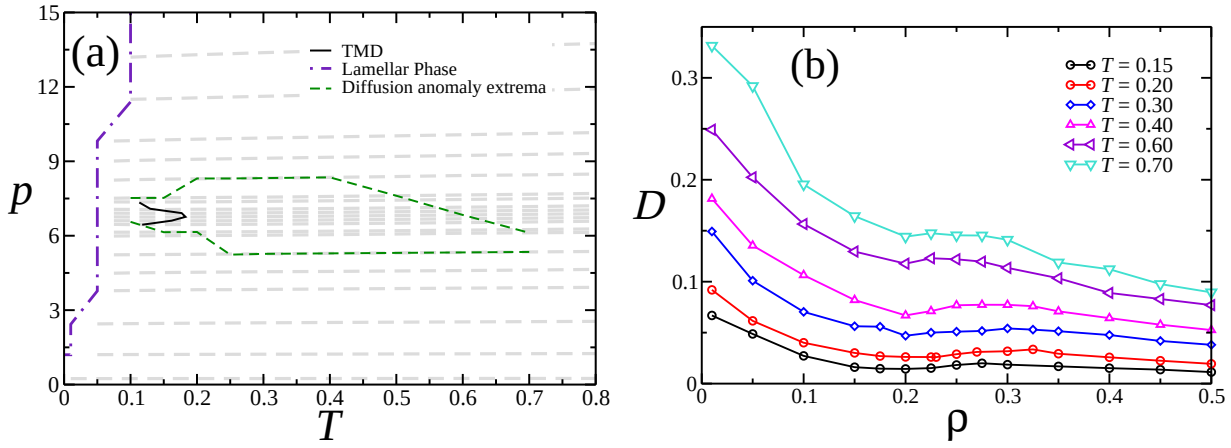

Figure 2: (a) $p \times T$ phase diagram for the system composed by A-B Janus nanoparticles. The black line denotes the TMD line, the dashed green line the diffusion anomaly region extrema and the dot-dashed purple line the separation between the fluid and the lamellar phase. Grey lines are the isochores. (b) Center of mass diffusion coefficient D as function of density ρ for different temperatures, showing the diffusion anomaly.

First, the system of Janus particles in which one monomer is of the type A and the other is of the type B, the AB system is analyzed. Previous works[42] have shown that dimers with two monomers of the type A exhibit thermodynamic, dynamical and structural waterlike anomalies and a liquid-crystal lamellar phase.

The pressure versus temperature phase diagram of this AB system is shown in the figure 2(a). In this system the density increases with the increasing temperature at constant pressure for certain values of pressure showing a maximum density. The temperature of maximum density for different pressures is illustrated as a solid line in the figure 2(a). The

points where obtained using equation 5 at the isochores illustrated as gray lines at the 2(a). The diffusion coefficient versus density for different temperatures is shown in the figure 2(b). For some temperatures, the diffusion coefficient, D, increases with ρ what characterizes an anomalous behavior. As a result for these temperatures there are a minimum and a maximum diffusion coefficient. The pressure and temperature of the maximum and minimum D forms two lines illustrated as dashed line in the figure 2(a). The region of the diffusion anomalous behavior in the pressure versus temperature phase diagram englobes the region of the density anomaly, i. e. the density anomalous regions is inside the diffusion anomalous region. This phenomena is identified as hierarchy of anomalies. This hierarchy is also observed for the monomeric[39] and A-A dimeric systems.[42]

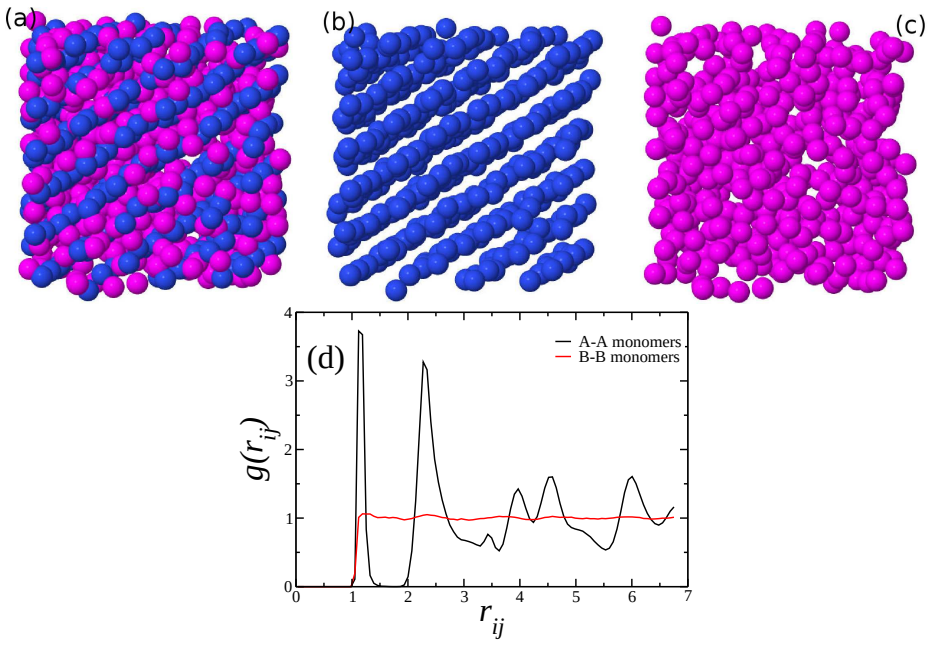

Figure 3: (a)System snapshot in the lamellar phase, at $T = 0.1$ and $\rho = 0.4$ including all particles, (b) only the A (blue) monomers and (c) only the B (pink) monomers. (d) Radial distribution function for A-A pairs (solid black line) and B-B pairs (solid red line).

The fluid-solid separation occurs at lower temperatures when compared with the dumbbell A-A case.[42] The asymmetry of the A-B Janus particle makes its solid easier to melt when compared with a less entropic A-A system. This solid phases in both A-A and A-B systems

were defined as the region where $D \approx 0$ and the fluid shows a well defined structure.

In the solid region of the pressure versus temperature phase diagram, the system is structured as lamellar phases as illustrated in the figure 3(a). It shows a snapshot of the nanoparticles at $T = 0.1$ and $\rho = 0.4$. In order to have a more clear visualization of the structure, the monomers A and B were analyzed separately. Figure 3(b) and (c) are snapshots of A monomers and B monomers, respectively. The monomers A are in a lamellar well defined structure, while the B monomers are disordered, with a fluid-like behavior. Since the center of mass diffusion coefficient is approximately null, this indicates that the A monomers are fixed in the lamellar structure, while the B monomers are spinning around the A monomers, in a fluid-like behavior. The radial distribution function for this point, shown in figure 3(d), reinforces this conclusion. The RDF for the A monomers is characteristic of a structured system while for the B monomers the RDF is clearly of a gas. For all densities and temperatures simulated only this lamellar structure was observed. The snapshots and RDF for this points are omitted for simplicity.

The hard sphere-two length scales dumbbell forms a plane of two length scales monomers as illustrated in the figure 3(b). In the case of a dumbbell in which both monomers interact through a two length scales potential the two monomers minimize the free energy by being apart a distance $d \approx 2\sigma$ between the lines. Inside each line the distance is $d_1 \approx 1\sigma$

The reason for this difference is that while the two length scales particles minimize the free energy being either at $d \approx 2\sigma$ e $d_1 \approx 1\sigma$, the hard core monomers are limited by the hardcore distance. The combination of these two particles that are linked by the dumbbell leads to the appearance of the planes.

Another effect from the Janus characteristic of the nanoparticle is that the liquid-crystal phase observed for A-A dimers was not observed in the A-B case. Once the anomalies are preserved, our results indicates that in the A-B case the two length scales potential dominates the fluid behavior.

A-C type nanoparticles

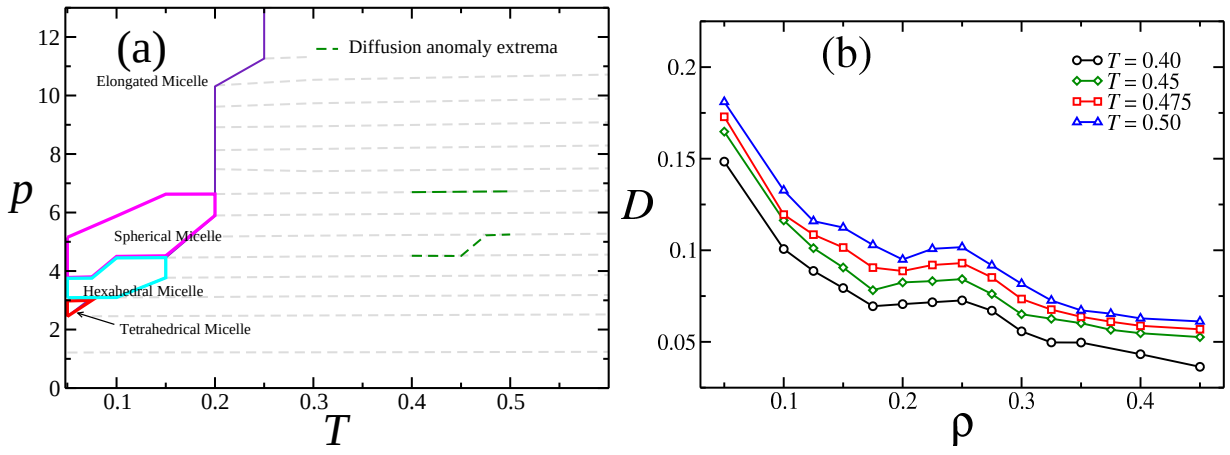

Figure 4: (a) $p \times T$ phase diagram for the system composed by A-C Janus nanoparticles. The dashed green line the diffusion anomaly region extrema and the distinct micellar regions are depicted in the graphic. Grey lines are the isochores. (b) Center of mass diffusion coefficient D as function of density ρ for different temperatures, showing the diffusion anomaly.

Next, the A-C Janus dimers were studied. Replacing the purely repulsive B monomer by the attractive C monomer leads to changes in the pressure versus temperature phase diagram when compared with the A-B case as illustrated in the figure 4. The figure 4(a) shows no minimum in the isochores and, therefore, no density anomaly is present. Figure 4(b) illustrated the diffusion coefficient versus density for fixed temperatures. The region in the pressure versus temperature phase diagram in which the diffusion anomaly is present is smaller (limited to the isotherms between $T = 0.4$ and 0.5)

The waterlike anomalies can be related with the competition between the two length scales (1).[24] As the temperature is increased the particles move away from the minimum of the potential to the closest length scale increasing the entropy while staying around the minimum of the potential, the second length scale, increases the enthalpy.[48] In this case, the suppression of the density anomalous region and the occurrence of diffusion anomaly only at high temperatures are consequences of the strong attractive interaction of the monomer C which favor the enthalpy against entropy.

Another difference between the A-B and the A-C nanoparticles are the self-assembled

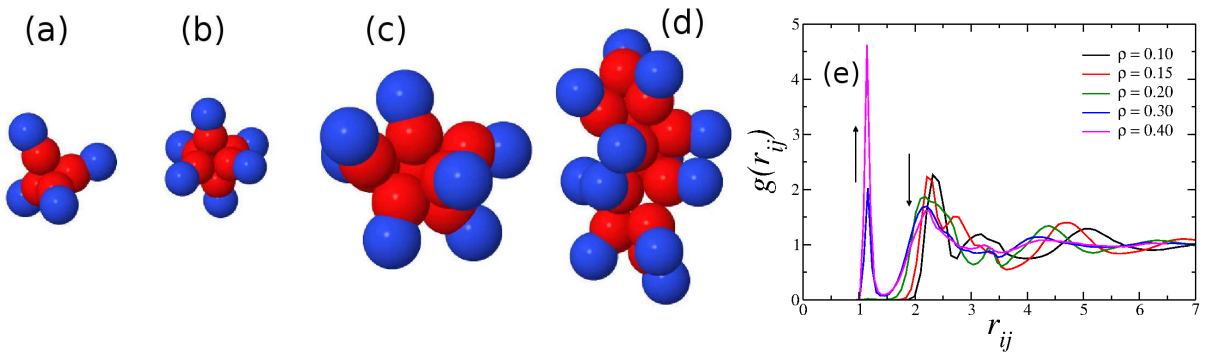

Figure 5: System snapshot in the micellar phase, at $T = 0.05$ and (a) $\rho = 0.10$, (b) 0.15, (c) 0.20 and (d) 0.30, respectively, showing the distinct self-assembled micelles: tetrahedral, hexahedron, spherical and elongated, form left to right. (e) Radial distribution function for A-A pairs at temperature $T = 0.05$ and for different densities, showing the competition between the length scales. The arrows indicates the behavior of each peak as the density increases.

structures that are formed. While for the first case only a lamellar phase was observed, for A-C monomers four different micellar structures were observed. In addition the micellation temperature for the A-C Janus system is higher than in the melting temperature for the A-B system. This result is not surprising since more attractive systems exhibits a higher melting temperature.

Figure 4(a) shows all the micellar phases. At $T = 0.05$ and lower pressures (the region illustrated as a red triangle in the figure 4(a)), the dumbbells are structured in a pyramidal tetrahedral clusters, similar to the water tetrahedral cluster, with the C monomers attached and pointing to the center of the cluster. Figure 5(a) show this structure for the density $\rho = 0.10$.

For higher pressures and $T = 0.05$, inside the region limited by the cyan line in the figure 4(a), the nanoparticles are in an hexahedron structure, composed by six dimers with the C monomers pointing to the center of the structure. This cluster is shown in the figure 5(b) for $\rho = 0.15$. Increasing the density, as $\rho = 0.20$, more dimers attach to the micelles, and the structure changes from a hexahedron to a spherical micelle. This structure was observed inside the region limited by the magenta line in figure 4(a). Finally, at even higher densi-

ties, as $\rho = 0.30$, the high pressure changes the micelles shape from spherical to elongated micelles, as shown in figure 5(c) and 5(d).

The transition between tetrahedral – hexahedron – spherical micelle can be understand by the fact that increasing the density (and consequently the pressure) more C monomers will be attached in a micelle, changing the structure shape. However, the spherical to elongated micelle transition is lead by the competition between the two length scales in the anomalous potential. The RDF between A monomers, displayed in figure 5(e), shows that, in the density range were the first three species of micelles were observed, all A monomers are at the second length scale, $r_{ij} \approx 2.0$, or further, while the first characteristic length scale, at $r_{ij} \approx 1.2$, do not have any occupancy. However, when the system is structured in elongated micelles the first length scale sharply increases, showing that the particles moved from the second length scale to the first one.

The presence of the self-assembled phases in the A-C Janus system not present in the A-B and A-A cases are not surprising. They also appear in the usual hydrophobic-hydrophilic Janus particles.[37] These phases are a result of the competition between the repulsion of the core-softened potential and the attraction of the LJ. As in the competing interaction models, all the transitions including the transition between the fluid to structured phases are first-order.

Conclusion

In this work we have analyzed the pressure versus temperature phase diagram of a Janus dumbbells system comparing the effects of the competition between two length scales potential and an repulsive and attractive potentials. Each nanoparticle was composed by one anomalous monomer modeled with a two length potential and one monomer modeled as a standard LJ particle.

We found that when the only competition is between the two length scales, the system

only shows the lamellar phase defined by the core-softened potential. In this case as in the pure CS dumbbell, density and diffusion anomalies are present in the pressure versus temperature phase diagram. In the case of he CS-attractive LJ dumbbell, the attraction affects the competition that lead to waterlike anomalies. As consequence, the density anomaly vanishes and the diffusion anomaly region shrinks. Also, the models shows a rich variety of micelles in self-assembly process similar to the behavior observed in the hydrophobic-hydrophilic Janus dumbbell. Due to the attraction between C monomers and the two length scales competition between A monomers the nanoparticles can assembly to tetrahedral, hexahedron, spherical or elongated micelles.

Our results indicated that is possible to create distinct colloidal particles that will have waterlike anomalies and different micellar conformation. Furthers investigations of Janus dumbbells, including distinct LJ well depthness, monomers size and separation, are currently in progress.

Acknowledgments

We thank the Brazilian agencies CNPq, INCT-FCx, and Capes for the financial support. We also thank to TSSC - Grupo de Teoria e Simulação em Sistemas Complexos at UFPel for the computational time in Satolep cluster.

References

(1) Talapin, D. M.; Lee, J.-S.; Kovalenko, M. V.; Shevchenko, E. V. Prospects of Colloidal Nanocrystals for Electronic and Optoelectronic Applications. *Che. Rev.* **2010**, *110*, 389–458.

(2) Elsukova, A.; Li, Z.-A.; Möller, C.; Spasova, M.; Acet, M.; Farle, M.; Kawasaki, M.; Ercius, P.; Duden, T. Structure, Morphology, and Aging of Ag–Fe Dumbbell Nanoparticles. *Phys. Status Solidi* **2011**, *208*, 2437–2442.

(3) Tu, F.; Park, B. J.; Lee, D. Thermodynamically Stable Emulsions Using Janus Dumbbells as Colloid Surfactants. *Langmuir* **2013**, *29*, 12679–12687.

(4) Walther, A.; Müller, A. H. E. Janus Particles. *Soft Matter* **2008**, *4*, 663–668.

(5) Boal, A. K.; Ilham, F.; DeRouchey, J. E.; Thurn-Albrecht, T.; Russel, T. P.; Rotello, V. M. Self-assembly of nanoparticles into structured spherical and network aggregates. *Nature* **2000**, *404*, 746–748.

(6) Glotzer, S. C.; Solomon, M. J.; Kotov, N. A. Self–Assembly: From Nanoscale to Microscale Colloids. *AIChE Journal* **2004**, *50*, 2978–2985.

(7) Kellu, G. S. Density, thermal expansivity, and compressibility of liquid water from 0.deg. to 150.deg.. Correlations and tables for atmospheric pressure and saturation reviewed and expressed on 1968 temperature scale. *J. Chem. Eng. Data* **1975**, *20*, 97–105.

(8) Angell, C. A.; Finch, E. D.; Bach, P. Spin?echo diffusion coefficients of water to 2380 bar and -20^oC. *J. Chem. Phys.* **1976**, *65*, 3063.

(9) Prielmeier, F. X.; Lang, E. W.; Speedy, R. J.; Lüdemann, H.-D. Diffusion in supercooled water to 300 MPa. *Phys. Rev. Lett.* **1987**, *59*, 1128.

(10) Chaplin, M. Seventh-two Anomalies of Water. `http://www.lsbu.ac.uk/water/anmlies.html`, 2014.

(11) Sastry, S.; Angell, C. A. Liquid-liquidphase transition in supercooled silicon. *Nature Mater.* **2003**, *2*, 739–743.

(12) Angell, C. A.; Bressel, R. D.; Hemmatti, M.; Sare, E. J.; Tucker, J. C. Water and its anomalies in perspective: tetrahedral liquids with and without liquid–liquid phase transitions. *Phys. Chem. Chem. Phys.* **2000**, *2*, 1559.

(13) Shell, M. S.; Debenedetti, P. G.; Panagiotopoulos, A. Z. *Phys. Rev. E* **2002**, *66*, 011202.

(14) Sharma, R.; Chakraborty, S. N.; Chakravarty, C. *J. Chem. Phys.* **2006**, *125*, 204501.

(15) Thurn, H.; Ruska, J. *J. Non-Cryst. Solids* **1976**, *22*, 331.

(16) *Handbook of Chemistry and Physics*, 65th ed.; CRC Press: Boca Raton, Florida, 1984.

(17) Sauer, G. E.; Borst, L. B. *Science* **1967**, *158*, 1567.

(18) Kennedy, S. J.; Wheeler, J. C. *J. Chem. Phys.* **1983**, *78*, 1523.

(19) Tsuchiya, T. *J. Phys. Soc. Jpn.* **1991**, *60*, 227.

(20) Cummings, P. T.; Stell, G. *Mol. Phys.* **1981**, *43*, 1267.

(21) Togaya, M. *Phys. Rev. Lett.* **1997**, *79*, 2474.

(22) Morishita, T. *Phys. Rev. E* **2005**, *72*, 021201.

(23) Chen, S.-H.; Mallamace, F.; Mou, C.-Y.; Broccio, M.; Corsaro, C.; Faraone, A.; Liu, L. *Proc. Natl. Acad. Sci. USA* **2006**, *103*, 12974.

(24) de Oliveira, A. B.; Salcedo, E.; Chakravarty, C.; Barbosa, M. C. Entropy, diffusivity and the energy landscape of a water-like fluid. *J. Chem. Phys.* **2010**, *132*, 234509.

(25) Yin, Y.; Lu, Y.; Xia, X. A Self-Assembly Approach to the Formation of Asymmetric Dimers from Monodispersed Spherical Colloids. *J. Am. Chem. Soc.* **2001**, *132*, 771–772.

(26) Singh, V.; Cassidy, C.; Grammatikopoulos, P.; Djurabekova, F.; Nordlund, K.; Sowwan, M. Heterogeneous Gas-Phase Synthesis and Molecular Dynamics Modeling of Janus and Core-Satellite Si–Ag Nanoparticles. *J. Phys. Chem. C* **2014**, *118*, 13869–13875.

(27) Lu, Y.; Yin, Y.; Li, Z.-Y.; Xia, Y. Synthesis and Self-Assembly of Au@SiO_2 Core–Shell Colloids. *Nano Lett.* **2002**, *2*, 785–788.

(28) Yoon, K.; Lee, D.; Kim, J. W.; Weitz, D. A. Asymmetric Functionalization of Colloidal Dimer Particles with Gold Nanoparticles. *Chem. Cummun.* **2012**, *48*, 9056–9058.

(29) Hu, J.; Zhou, S.; Sun, Y.; Fang, X.; Wu, L. Fabrication, Properties and Applications of Janus Particles. *Chem. Soc. Rev.* **2012**, *41*, 4356–4378.

(30) Li, M.; Schnablegger, H.; Mann, S. Coupled synthesis and self-assembly of nanoparticles to give structures with controlled organization. *Nature* **1999**, *402*, 393–395.

(31) Song, Y.; Klivansky, L. M.; Liu, Y.; Chen, S. Enhanced Stability of Janus Nanoparticles by Covalent Cross-Linking of Surface Ligands. *Langmuir* **2011**, *27*, 14581–14588.

(32) Takahara, Y. K.; Ikeda, S.; Ishino, S.; Tachi, K.; Ikeue, K.; Sakata, T.; Hasegawa, T.; Mori, H.; Matsumura, M.; Ohtani, B. Asymmetrically Modified Silica Particles: A Simple Particulate Surfactant for Stabilization of Oil Droplets in Water. *J. Am. Chem. Soc.* **2005**, *127*, 6271–6275.

(33) Liu, J.; Liu, G.; Zhang, M.; Sun, P.; Zao, H. Synthesis and Self–Assembly of Amphiphilic Janus Laponite Disks. *Macromolecules* **2013**, *46*, 5974–5984.

(34) Milinković, K.; Dennison, M.; Dijkstra, M. Phase Diagram of Hard Asymmetric Dumbbell Particles. *Phys. Rev. E* **2013**, *87*, 032128.

(35) Bianchi, E.; Likos, C. N.; Kahl, G. Tunable Assembly of Heterogeneously Charged Colloids. *Nano Lett.* **2014**, *14*, 3412–3418.

(36) Carey Bagdassarian, A. B.-S., William M. Gelbart Liquid crystalline states of surfactant solutions of isotropie micelles. *Journal of Statistical Physics* **1988**, *52*, 1307–1313.

(37) Liu, Y.; Li, W.; Perez, T.; Gunton, J. D.; Brett, G. *Langmuir* **2012**, *28*.

(38) Barbosa, M. C. Influence of Fluctuations on Spin Systems with Spatially Isotropic Competing Interactions. *Phys. Rev. B* **1990**, *42*, 6363.

(39) de Oliveira, A. B.; Netz, P. A.; Colla, T.; Barbosa, M. C. Thermodynamic and Dynamic Anomalies for a Three Dimensional Isotropic Core-Softened Potential. *J. Chem. Phys.* **2006**, *124*, 084505.

(40) Allen, P.; Tildesley, D. J. *Computer Simulation of Liquids*; Oxford University Press, Oxford, 1987.

(41) de Oliveira, A. B.; Netz, P. A.; Colla, T.; Barbosa, M. C. Structural anomalies for a three dimensional isotropic core-softened potential. *J. Chem. Phys.* **2006**, *125*, 124503.

(42) de Oliveira, A. B.; Nevez, E.; Gavazzoni, C.; Paukowski, J. Z.; Netz, P. A.; Barbosa, M. C. Liquid crystal phase and water-like anomalies in a core-softened shoulder-dumbbells system. *J. Chem. Phys.* **2010**, *132*, 164505.

(43) Kell, G. S. NO TITLE. *J. Chem. Eng. Data* **1967**, *12*, 66.

(44) Angell, C. A.; Finch, E. D.; Bach, P. Spin-Echo Diffusion Coefficients of Water to 2380 bar and ÃćÂĹÂŠ20^{o}C. *J. Chem. Phys.* **1976**, *65*, 3063–3066.

(45) Ryckaert, J. P.; Ciccotti, G.; Berendsen, H. J. C. *J. Comput. Phys.* **1977**, *23*, 327.

(46) Limbach, H.-J.; Arnold, A.; Mann, B. A.; Holm, C. ESPResSo - An Extensible Simulation Package for Research on Soft Matter Systems. *Comput. Phys. Commun.* **2006**, *174*, 704–727.

(47) Arnold, A.; Lenz, O.; Kesselheim, S.; Weeber, R.; Fahrenberger, F.; Roehm, D.; KoÅąovan, P.; Holm, C. In *Meshfree Methods for Partial Differential Equations VI*; Griebel, M., Schweitzer, M. A., Eds.; Lecture Notes in Computational Science and Engineering; Springer Berlin Heidelberg, 2013; Vol. 89; pp 1–23.

(48) de Oliveira, A. B.; Netz, P.; Barbosa, M. C. An ubiquitous mechanism for water-like anomalies. *Europhys. Lett.* **2009**, *85*, 36001.

Graphical TOC Entry